Front. Earth Sci. 2016, 10(1): 126–134
DOI 10.1007/s11707-015-0507-6

RESEARCH ARTICLE

Influence of climatic factors on tree-ring maximum latewood density of *Picea schrenkiana* in Xinjiang, China

Yu SUN[1,2], Lili WANG (✉)[1], Hong YIN[3]

1 Key Laboratory of Land Surface Pattern and Simulation, Institute of Geographic Sciences and Natural Resources Research, Chinese Academy of Sciences, Beijing 100101, China
2 University of Chinese Academy of Sciences, Beijing 100049, China
3 National Climate Center, China Meteorological Administration, Beijing 100081, China

Abstract The influence of temperature and precipitation on maximum latewood density (MXD) was mainly discussed in this paper, based on the samples of *Picea schrenkiana* from the Manas River Basin, Xinjiang, China. The correlation analysis between MXD and instrumental records from the Shihezi Meteorological Station showed that the MXD was positively related to the mean maximum temperature throughout the growing season at high elevations. Comparatively, the ring-width at low altitudes was limited by the precipitation in May–June. The composite chronology by MXD sequences was highly correlated with the mean maximum temperature in July–August ($r = 0.54$, $p < 0.001$), which was then reconstructed by the composite chronology. The comparative analysis on the reconstructed temperatures, observed values, and drought indices (*Is*) revealed that precipitation would affect MXD when the absolute value of Is was greater than 1.5σ (i.e., $|Is| > 2.5$) in the period of 1953–2008 A.D. or close to 1.5σ for 2–3 consecutive years. The response characteristics are linked with the semiarid climate in the study area. In a single year or consecutive years of extreme dryness, the lack of precipitation would limit the thickening of latewood cell walls and thus impact the MXD. All in all, if a MXD chronology is aimed to reconstruct temperature history, the moisture conditions at the sampling site should be considered prudently.

Keywords *Picea schrenkiana*, tree-ring, maximum latewood density, air temperature, precipitation

Received July 25, 2014; accepted October 29, 2014

E-mail: wangll@igsnrr.ac.cn

1 Introduction

Recently, great advances have been achieved in China in terms of longer or super-long series construction and research depth and breadth. On the northeastern Tibetan Plateau, the tree-ring width chronology of *Sabina przewalskii Kom.* was extended to about 4,000 years ago, which precisely indicated wet and dry changes in the region (Shao et al., 2010; Yang et al., 2014). Tree rings of *Sabina tibetica Kom.* recorded the past 600-year temperatures with high resolution, the longest so far on the central Tibetan Plateau (He et al., 2014). In Northeast China, the long temperature reconstruction implicated the dynamics of the East Asian winter monsoon (Zhu et al., 2009), whereas the decreased sensitivity of tree growth to temperature in Southeast China was linked to the regime shift in the Pacific climate (Wang et al., 2014).

Accompanied by the rapid development of ring-width research, researchers at home and aboard are conducting valuable research on climate change by means of maximum latewood density (MXD). Summer temperatures have been reconstructed in Western Europe (Briffa et al., 1988), America (Schweingruber et al., 1991) and Alberta, Canada (Luckman et al., 1997). In China, Fan et al. (2009) reconstructed the summer temperatures in the middle of Hengduan Mountains and Duan et al. (2010) calculated the August–September mean temperature on the eastern Tibetan Plateau. All the close relationships between MXD and temperature were revealed in high-latitude or high-altitude and relatively humid regions. Therefore, there is need to evaluate the MXD/climate pattern at semiarid sites. The influence of precipitation on the MXD as another key climatic factor to tree growth was seldom discussed before and only involved in a few of biological researches (Wimmer and Grabner, 2000; Gruber et al., 2010). In some tree-ring research, a negative correlation

was found between MXD and precipitation because temperature, negatively correlated with precipitation, positively limited the MXD. Thus, the actual direct physiological relation between MXD and precipitation couldnot be explained.

This paper, taking the *Picea schrenkiana* growing in semiarid climates, discusses the impact of temperature and precipitation on MXD in detail on a physiological view. The analysis of the MXD/climate relationship will be a great help for proper site selection when researchers utilize MXD to reconstruct paleoclimate.

2 Materials and methods

2.1 Overview of the study area

The forest region in the middle of Tianshan Mountains stands to the southern margin of Junggar Basin, stretching more than 800 km with a peak elevation of 4,000−5,000 m a.s.l. (above sea level). The *Picea schrenkiana* forest in the area exists at 1,650−2,850 m a.s.l. With the Gurbantunggut Desert to the north, and far from the ocean, this forest lies in the continental climate zone, with prominently arid sunny slopes and much rainfall only in the mid-mountains. Running from south to north, the Manas River is the largest snowmelt river on the southern margin of Junggar Basin, with a total length of 324 km and multi-year mean runoff of 11.9×10^8 m^3. In the Shihezi reclamation area, winters are long and cold, but summers are short and hot. The annual mean temperature is 7.5°C–8.2°C, the mean altitude is 300−500 m a.s.l., the sunshine duration is 2,318−2,732 h, the frost-free period is 147−191 d, and the annual rainfall is 180−270 mm (Comprehensive Expedition of Chinese Academy of Sciences in Xinjiang, 1958; Zhang, 2006). *Picea schrenkiana* were sampled in August, 2009, from Meiyaogou (MYG), Dashuwan (DSW) and Lucaogou (LCG). The detailed information on those sampling sites is showed in Table 1 and the location and terrain are profiled in Fig. 1.

2.2 Research approaches

In the wild, 10-mm-diameter increment borers were used to extract the cores of *Picea schrenkiana* at the breast height and perpendicular to the slope aspect. Two cores were typically taken from each tree. The samples were taken back in paper straws, fixed by standard procedures (Cook and Kairiukstis, 1990) in the lab, and then polished and visually dated for the tree rings after being air-dried. Next, the ring-width data were obtained by the LINTAB measuring apparatus with a resolution of 0.01mm, and they were cross-dated and finally checked with the TSAP and COFECHA programs (Cook et al., 2000) carefully.

After measurement and cross-dating of ring-widths, the

Table 1 Information of sampling sites

Site	Code	Elevation/m	Latitude/N	Longitude/E	Aspect	Sample depth (trees/cores)
Lucaogou	LCG	2,494	43.82°	85.89°	N	24/46
Dashuwan	DSW	2,059	43.84°	86.03°	N	25/49
Meiyaogou	MYG	1,987	43.82°	86.07°	N	24/48

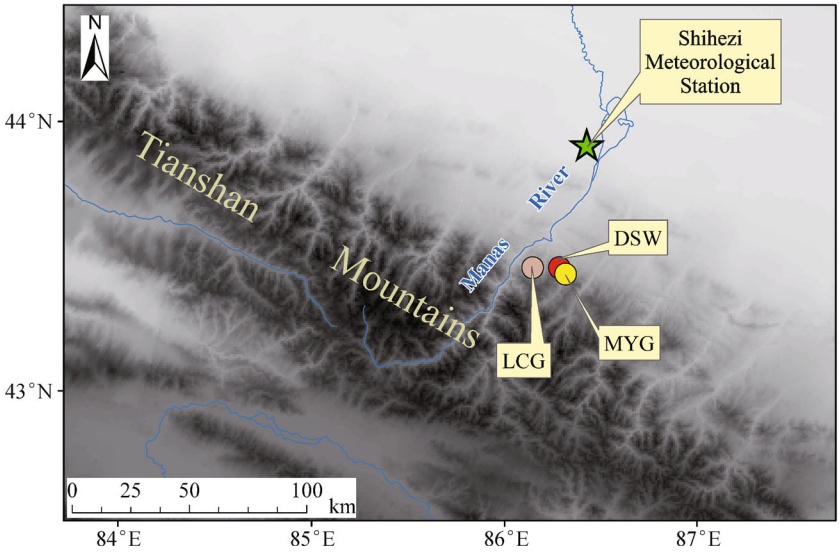

Fig. 1 Map of sampling sites and the meteorological station.

samples were prepared for density analysis. Following standard practices (Lenz et al., 1976; Schweingruber et al., 1988), all the cores were cut into sections and the angles of wood fibers were measured with Dendroscope. The Dendro2003 system was subsequently used to cut the sections into laths 1.0 mm thick, take X-ray films and measure the grey-scale variations to get tree-ring densities by transforming the optical strength. The earlywood width, latewood width, earlywood average density, latewood average density, minimum earlywood density, MXD and total tree-ring width (TRW) were obtained. The cross-dating of tree-ring densities was conducted according to the well dated ring-widths, and the cross-dating quality of ring-densities was also tested utilizing the TSAP and COFECHA programs to ensure the accuracy.

MXD and TRW chronologies were developed with the ARSTAN program (Cook, 1985). By comparative analysis on raw measurements and repeated attempts on various fitting methods, the smoothing spline with two thirds of the series length was selected to eliminate or diminish the influence of disturbances and variations in the development of MXD with age, and the growing trend of TRW was fitted by the smoothing spline with the step of sixty years. With better performance in statistics and higher correlation with climatic factors than other kinds of chronologies, the standardized index series of MXD and TRW at the three sampling sites were established and chosen for a further analysis. Three TRW chronologies were presented in Fig. 2. Because of the lowest correlation and shortest length, the MXD standard chronology of MYG was inconsistent with the other two MXD chronologies, while the MXD chronologies of DSW and LCG showed more similar changes and significant relationship ($r = 0.616$, $n = 188$ yr, $p < 0.001$). Thus, all MXD series of DSW and LCG were combined to construct a composite chronology (the Composite Chronology is referred to as "CC" hereinafter) after rechecking the uniformity with the COFECHA program and deleting those irrelevant sequences. Figure 3 shows four MXD chronologies and Table 2 illustrates the statistical results of each chronology in the common interval.

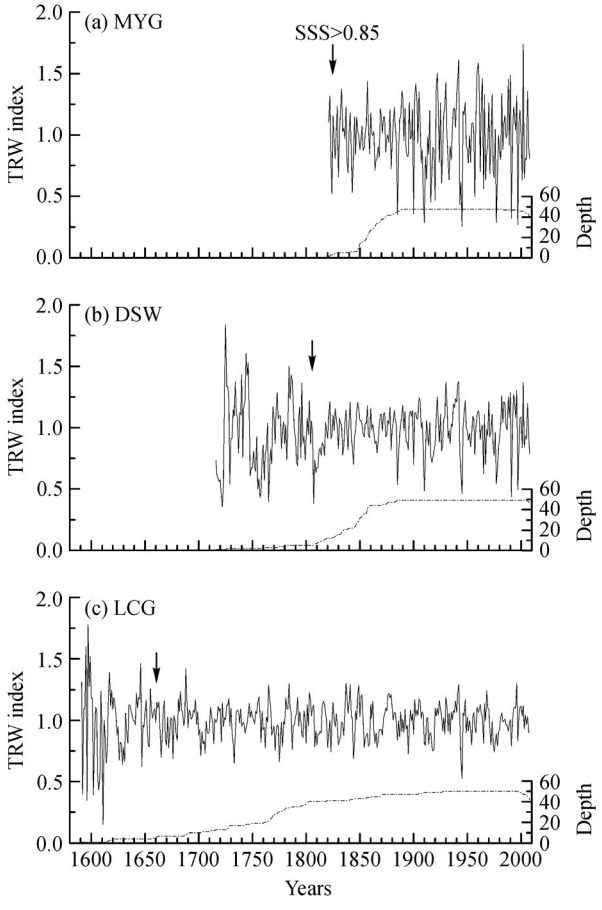

Fig. 2 TRW chronologies of MYG (a), DSW (b) and LCG (c).

2.3 Meteorological data

Four monthly parameters were selected from the Shihezi Meteorological Station, which is closest to the sampling sites: precipitation (Pre), mean temperature (Tem), mean maximum temperature (Max) and mean minimum temperature (Min). The data from 1953 to 2008 A.D. were downloaded from the China Meteorological Data Sharing Service System (http://cdc.cma.gov.cn/). Shihezi Meteorological Station, situated at 86°03′E and 44°19′N, is a national principal station without any migrating history, and its observation field is 442.9 m a.s.l. All the meteorological data were normalized and no abnormal value was found when the data was rechecked. The 56-year monthly mean precipitation and temperature recorded by the Shihezi Meteorological Station were drawn in Fig. 4. Looking at Fig. 4, the study area belongs to a semiarid region. The precipitation mostly falls in April and May, the early growing season, and decreases in July−September, the late growing season. In contrast, the temperature is highest in June−August, asynchronous with the precipitation.

3 Results and discussion

3.1 Correlation between TRW/MXD and climatic factors

The MXD and TRW chronologies were used to make a correlation analysis with four climatic factors, including the Pre, Max, Tem, and Min, from October to October. The results are shown in Figs. 5 and 6; grey bars indicate the significantly correlated months.

In Fig. 5, the relationship between the chronology of MYG and climatic elements is quite different from those between the others and the meteorological data. For the other three chronologies, the correlations between any

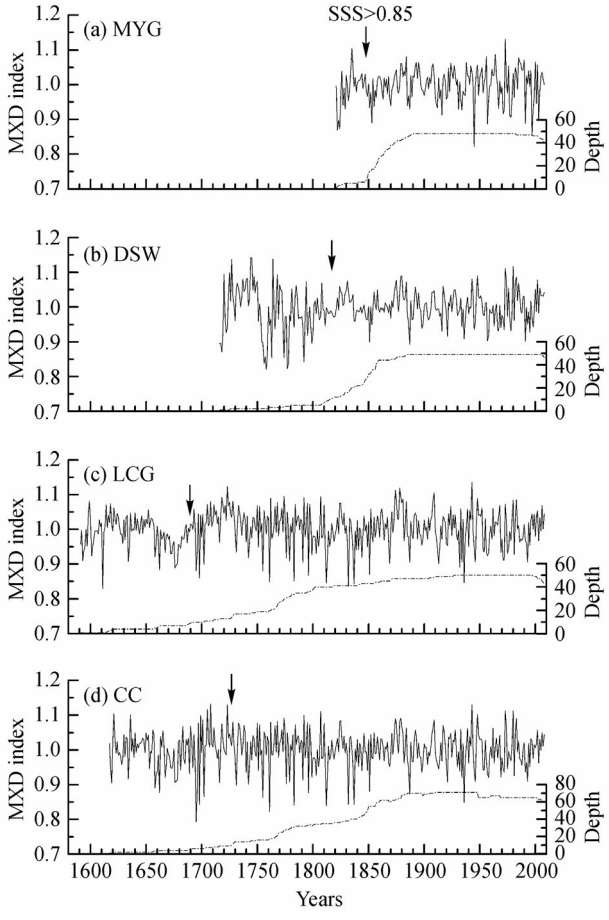

Fig. 3 MXD chronologies of MYG (a), DSW (b) and LCG (c) and the composite MXD chronology (d).

chronology and the Pre in each month are not significant. However, the changing trends of correlation coefficients are relatively uniform, perhaps implying that the effect of Pre on MXD is roughly similar. On the other hand, the associations between the other three chronologies and temperature resemble each other as well, closest to the Max in August, followed by the Min in May. The positive correlation means the higher the temperature, the greater the MXD.

Since the process of tree growth is continuous, the correlation between MXD chronologies and climatic factors in the combined months should be checked. The averages of temperature and the sums of precipitation were calculated in May–August and July–August respectively, due to their relatively high correlations. The results showed that the CC was closest to the Max in July–August. Consequently, the key limiting factor to MXD is the Max in July–August, the dominant growing stage. The most critical period for cell walls to thicken is from the concurrent July to August, which has been shown in past research (Chen et al., 2009).

In May, the highest rainfall arrives at the Shihezi region (Fig. 4). Rapid rises in the Min make the growing season begin earlier and last longer. During these situations, trees can accumulate adequate substance to thicken cell walls, forming greater MXDs (Chen et al., 2009). The main growing season of *Picea schrenkiana* is from May to August (Lu and Yan, 1990) and therefore, in the late part of growing season, July–August, the fission and elongation of cells almost finish, the new leaves mature, and the photosynthetic accumulation begins. Hence, radial growth of trees mainly occur in the thickening of latewood cell walls (Greber and Chaloner, 1984).

In the growing season, the Max plays a significant role in forming the MXD and becomes the restricting factor to the MXD, especially in July–August (Chen et al., 2009). *Picea schrenkiana* is thought to be photophilous or light-resistant, for the reason of dilution process or lack of pioneer species in the history. Besides, the trees require full light conditions in the fast-growing stage after they are more than 25 years old (Lu and Yan, 1990). Full light often generates high temperature, which is perhaps the indirect

Table 2 Summary statistics of STD chronologies (the common interval: 1850–2000 A.D.)

Item	TRW			MXD			
	MYG	DSW	LCG	MYG	DSW	LCG	CC
Mean sensitivity	0.332	0.195	0.153	0.050	0.045	0.055	0.061
Standard deviation	0.290	0.228	0.172	0.050	0.055	0.053	0.057
1st-order coefficient of autocorrelation	0.040	0.452	0.232	0.167	0.398	0.115	0.078
SSS > 85% year/cores	1825/3	1808/6	1661/6	1848/8	1819/12	1689/9	1727/10
All series rbar	0.692	0.481	0.467	0.391	0.256	0.343	0.372
Between-trees rbar	0.688	0.476	0.460	0.386	0.251	0.337	0.369
Within-trees rbar	0.859	0.729	0.789	0.604	0.491	0.595	0.611
Signal to noise ratio	103.4	45.4	40.3	29.5	16.9	24.0	36.2
Expressed population signal	0.990	0.978	0.976	0.967	0.944	0.960	0.973
Variance of 1st PCA/%	71.2	53.0	48.7	42.6	32.3	37.4	39.0

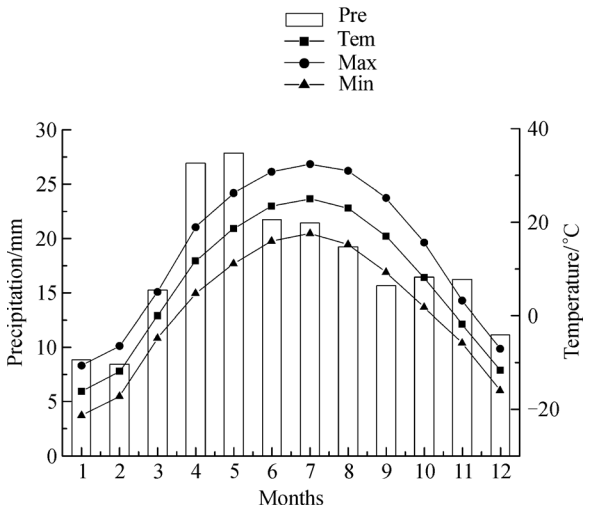

Fig. 4 Monthly mean precipitation and temperature from Shihezi Meteorological Station (1953–2008 A.D.).

reason why the Max could promote the development of MXD.

Apparently, MXD is more sensitive to the temperature. However, the response features of TRW are quite different from those of MXD. In the research area, at high altitude, the temperature decreases sharply, whereas the precipitation increases. MYG, located at the lowest elevation, is characterized by a warmer and drier climate than the other two sites. In Fig. 6, the TRWs of MYG and DSW are positively correlated with the Pre in June and May–June. Since high temperature could promote the evaporation of precipitation, the TRW of MYG and DSW is influenced by the temperature indirectly. TRW seems to show stronger sensitivity to the Pre than MXD does.

The correlation between the TRW chronologies of DSW, the middle site, and MYG, the lowest site, is higher (r = 0.835, n = 184) because the TRWs are strongly limited by the precipitation. However, as the limiting factor to TRW in May–June, precipitation increases with higher altitude. Therefore, the TRW chronology of LCG, the highest site, shows lower correlation with that of DSW (r = 0.640, n = 184).

On the other hand, the MXD chronology of DSW exhibits a closer association with LCG (r = 0.685, n = 161) than with MYG (r = 0.655, n = 161), since the temperature is not the limiting factor to MXD at the lowest altitude. Hence, the MXD variation of MYG, the lowest and warmest site, is inconsistent with the other two, even though MYG is located nearer to DSW than LCG is.

3.2 Influence of extreme changes in moisture conditions on MXD

In order to illustrate the response of MXD to temperature changes and to screen out the influence of moisture

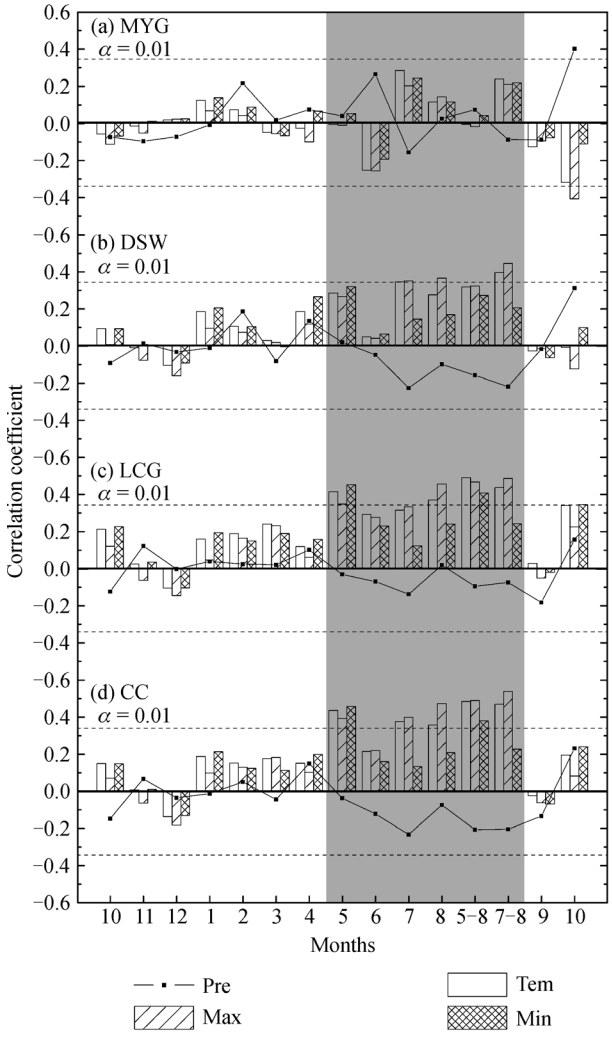

Fig. 5 Results of Person Correlation Analysis between MXD chronologies and instrumental records from Shihezi Meteorological Station (1953–2008 A.D.).

conditions on MXD, the equation of linear regression between CC and the Max in July–August was written as: T_{7-8}= 10.648CC + 21.220, where T_{7-8} stands for the reconstructed Max in July–August and CC means the composite MXD chronology. The calibration period of the equation is from 1953 to 2008. Statistics of the transfer equation and the leave-one-out cross validation are listed in Table 3, which clearly shows that the explained variance and other statistics are imperfect even though the correlation coefficient is significant at the 0.001 level.

To highlight the effect of precipitation on MXD, the drought index was selected and calculated as follows:

$$Is = \frac{R-\overline{R}}{\sigma_R} - \frac{T-\overline{T}}{\sigma_T}.$$

Is is the homogenized index of precipitation and temperature (Kite, 1977), namely the difference between

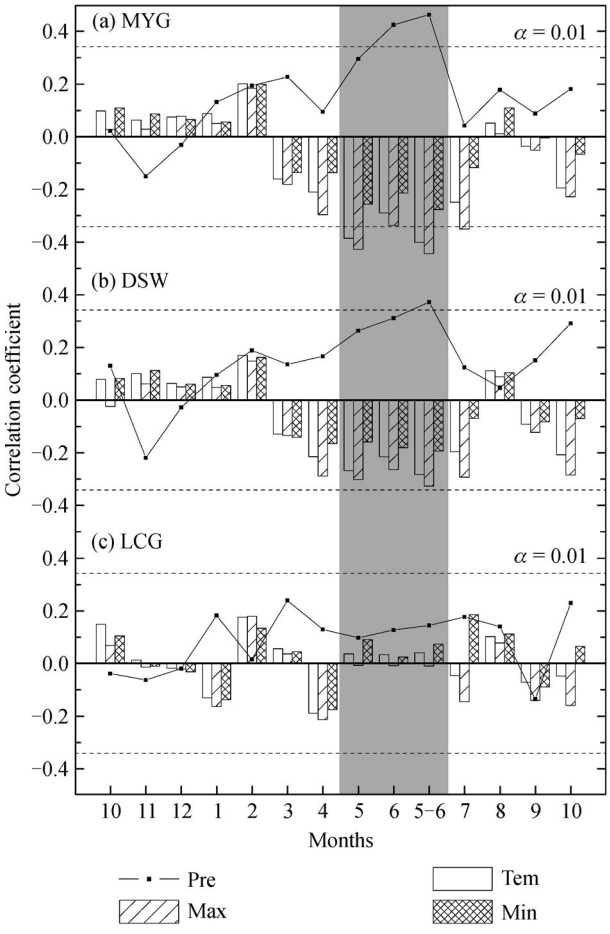

Fig. 6 Results of Person Correlation Analysis between TRW chronologies and instrumental records from Shihezi Meteorological Station (1953−2008 A.D.).

standardized precipitation and standardized temperature; R stands for the sum of precipitation in July-August; $\overline{R}$ epresents the multi-year average of R; σ_R means the standard deviation of R; likewise, T denotes the mean maximum temperature in July−August; $\overline{T}$ is the multi-year average of T; σ_T signifies the standard deviation of T.

The homogenized index of precipitation and temperature was chosen because it could indicate distinctly two extreme states, namely dryness with high temperature (negative *Is*) and wetness with low temperature (positive Is), and respond quickly to the fluctuations of precipitation and temperature (Kite, 1977), which were in line with the research aim.

The drought indices, reconstructed temperatures, and observed values were contrasted in Fig. 7, and the grey shades highlighted the periods when the absolute values of drought indices were extremely high (greater than 1.5σ, $|Is| > 2.5$) or continuously high over a 3-year period (close to 1.5σ). In these intervals (1958−1961, 1967, 1974−1976, 1985−1987, and 1996−1998), the calibration exhibited an obvious distance from the observed values.

As recorded, the runoff of the Manas River near the sampling points, was larger in 1958 and 1967, indicating the wetter years, while smaller in 1974−1976 and 1985−1987, indicating drier years (Yuan et al., 2007). Additionally, it was reported that strong deluges invaded the cities and counties in the study area in July and August, 1958 and 1959, and that severe droughts occurred in 1974, 1976, 1985−1987 and 1997 (Shi, 2006). The corresponding runoff records, disaster history, and drought indices further proved that there were great changes in moisture conditions during these years. Thus, these years were discarded from the original calibration period and cross validation was made again. In Table 3, the explained variance has been improved remarkably; *RE* is 0.4041, higher than the quondam 0.2450; t is 2.9310, better than 2.9088 in the overall calibration period; both the sign test and first difference sign test reach the 99% confidence level, stating the excellent consistency between the reconstructed Max in July−August and instrumental records at both high and low frequencies. The original model only reaches the 95% confidence level in the first difference sign test, with poor effect. The improvement of statistics showed that moisture conditions exerted a large influence on the MXD in 1958−1961, 1967, 1974−1976, 1985−1987 and 1996−1998, and showed both why MXD couldn't capture the changes in temperature precisely, and the fitting quality of the original

Table 3 Calibration and verification of the transfer equation between CC and $T_{7\text{-}8}$

	1953−2008	Years except 1958−1961, 1967, 1974−1976, 1985−1987, and 1996−1998
Explained variance/%	29.2	46.7
Adjust explained variance/%	27.9	45.3
F	22.3	35.0
First difference sign test	37*	30**
Sign test	40**	32**
t	2.9088	2.9310
Reduction error	0.2450	0.4041
r	0.50	0.64
p	< 0.001	< 0.001

* Means significant correlation at the 0.05 level; ** means significant correlation at the 0.01 level.

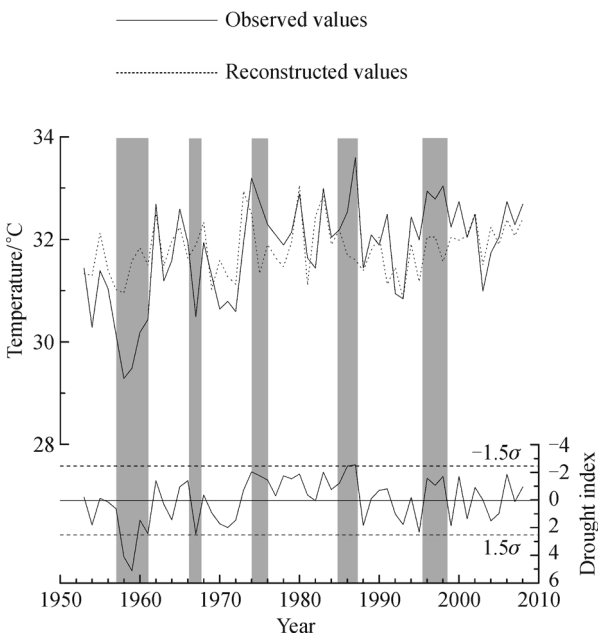

Fig. 7 Comparison among the reconstructed Max, observed Max, and drought indices in July−August.

model was not ideal. If these intervals were removed, MXD would become a fairly accurate temperature proxy.

The correlation coefficient between the *Is* and MXD is −0.445 ($n = 56$ yr, $p < 0.001$); however it cannot be used to truly reflect the effect of moisture conditions on MXD. The MXD is negatively correlated with Pre (not significant) and positively with Max ($\alpha = 0.01$) in July−August. Also, the drought index is the difference between standardized sequences of precipitation and temperature. Therefore the drought index is negatively linked with the MXD. In the calibration period, the influence of temperature on MXD is remarkable. Hence, when it comes to the effect of precipitation on MXD, it should be considered how moisture changes offset the MXD to express the temperature information with deviation, namely the relationship between the drought indices and the differences of reconstructed Max and observed values (D-value). The correlation coefficient between the *Is* and D-value is 0.699 ($n = 56$ yr, $p < 0.001$) in the overall calibration period, while it rises to 0.932 ($n = 14$ yr, $p < 0.001$) in 1958−1961, 1967, 1974−1976, 1985−1987 and 1996−1998. Correlation analysis, combined with the qualitative analysis in Fig. 7, fully demonstrates that the bigger the positive *Is*, the wetter the study area, and the greater the positive D-value and MXD tend to be.

3.3 Physiological explanation of the influence of moisture on MXD

The physiological mechanism of the influence of precipitation on MXD has seldom been discussed. Thus, here, we try to give some clues into four aspects of this issue. The third and forth points are only hypotheses.

Firstly, according to previous microscopic studies, drought stress could suppress the expansion of tracheids in the initial stage of growing season (Greber and Chaloner, 1984). If the cells are small in dimension, the proportions of cell walls will increase, leading to greater tree-ring densities, especially the earlywood densities (Pant et al., 2000; Chen et al., 2010). However, the key impact factor on MXD is the climate condition in the late growing season, when cell elongation has largely stopped. The MXD is determined by the thickness of cell walls rather than the size of cells (Yasue et al., 2000). If there is more precipitation after the summer solstice, the time for the development of latewood will be extended, resulting in wider latewood and thicker latewood cell walls (Wimmer and Grabner, 2000). On the contrary, in dry conditions, cambial activities end early, which shortens the time for the development of wood (Pichler and Oberhuber, 2007; Gruber et al., 2010). Besides, stronger water requirements and less water supplies order the stomatal closure, reducing the air exchange and carbon fixation (Jones, 1998). Meanwhile, more carbon will be supplied and stored for the root growth (Dewar et al., 1994; Wiley and Helliker, 2012). Eventually, both the substance and time for thickening cell walls are lessened, leading to thinner cell walls (Irvine et al., 1998; Cinnirella et al., 2002; Piovesan et al., 2008).

Secondly, on an ecological perspective, *Picea schrenkiana* appears to be a hygrophilous species. If the relative humidity is lower than 50% in summer, it is hard for *Picea schrenkiana* to live (Lu and Yan, 1990). Under hot and dry conditions, though heavy irrigation is adopted to maintain adequate soil moisture, water loss by intensive transpiration, resulting from the dry air cannot be replenished (Lu and Yan, 1990). Water plays an important physiological role in plants (Zhang et al., 2015). It is because of the strong dependency of *Picea schrenkiana* on moisture and the significant role of water that the extreme changes in precipitation could easily affect the physiological activities of trees, causing variations in MXD.

In addition, water is one of the basic materials for photosynthesis. However, the water needed for photosynthesis is only a small amount of all that is absorbed by plants (below 1%). Thus, the lack of water decreases the photosynthesis rate indirectly. Specifically speaking, leaves will close their stomata in case of aggravating water shortage, reducing the stomata conductance, which weakens the supply function of photosynthesis. At the same time, water shortage could promote amyl hydrolysis and accumulation of sugar in leaves. The slow output of photosynthetic products will cut down the demand function of photosynthesis (Lambers et al., 2008). Such two-sided reasons could reduce the substance required for thickening cell walls and at length, lead to smaller MXDs.

Finally, phytohormones could drive the cell growth by regulating the elongation of cell walls. Presently, the

phytohormones are thought to regulate the reshaping of polysaccharides net structures of cell walls by activating the expression of relaxation factors, and eventually cell walls are expanded (Miedes et al., 2011). For example, auxin can rapidly increase extensibility of cell walls (Swarup et al., 2008) and some genes related to cell walls are controlled by ethylene (Nemhauser et al., 2006). Although there is no clear report on the mechanism of effect of plant hormones on the thickening of cell walls, plant hormones do play a significant role in the material synthesis, decomposition, and microtubules arrangement of cell walls (Yuan et al., 1994). In extremely dry or humid conditions, the feedback response, such as the changes in quantity and transfer of various hormones, would act in plants (Lambers et al., 2008). Hormones are likely to curb the substance accumulation of cell walls through synergistic and antagonistic actions, changing the MXD on the appearance. Currently, hormones are sure to control the transfer of tree-ring development from earlywood to latewood (Uggla et al., 2001). Although it is unclear whether plant hormones could cause the changes in MXD, the relationship is probably close.

Since few studies have been made, we tried to discuss the impact of precipitation on MXD on a physiological view. Two of the four points mentioned above are hypotheses and we hope to raise some other thoughts on the issue. This study may also provide new insights on the restricting threshold of precipitation to MXD, and researchers should be careful when they reconstruct paleoclimate by MXD chronologies.

4 Conclusions

In this paper, we presented a composite MXD chronology with the mixture of signals inside. Under such climate pattern, MXD is not only controlled by temperature, but also could be interfered with by extraordinary moisture conditions. Hence, MXD is not suitable for paleoclimate reconstruction by current technological means in this case.

Main outcomes are as follows:

1) Along the Manas River in the Shihezi region, the MXD of *Picea schrenkiana* is mainly limited by the mean maximum temperature in July−August at high elevations. Relatively, TRW is more sensitive to precipitation and restricted by that in May−June at low altitudes.

2) When the absolute values of drought indices are greater than 1.5σ (i.e., $|Is| > 2.5$) of the period 1953−2008 AD or close to 1.5σ in a 3−year period, the precipitation would interfere MXD, which is related to the semiarid climate in the research area.

3) In dry years, the lack of water would change MXD by restricting the thickening of cell walls. Accordingly, the response of MXD to temperature in semiarid regions would be influenced by extreme moisture conditions, and as a temperature proxy, MXD should be applied prudently and limitedly.

Acknowledgements This research was supported by the National Natural Science Foundation of China (Grant Nos. 41275120, 41271120, and 41301041) and "135" Strategic Research Project of IGSNRR, CAS (No. 2012ZD001). Ring-density experiment supports from the Laboratory for Climate Studies, China Meteorological Administration are also appreciated.

References

Briffa K R, Jones P D, Schweingruber F H (1988). Summer temperature patterns over Europe: a reconstruction from 1750 A.D. based on maximum latewood density indices of conifers. Quat Res, 30(1): 36–52

Chen F, Yuan Y J, Wei W S, Yu S L, Li Y, Zhang R B, Zhang T W, Shang H M (2010). Chronology development and climate response analysis of Schrenk Spruce (*Picea schrenkiana*) tree-ring parameters in the Urumqi River Basin, China. Geochronometria, 36(1): 17–22

Chen J, Wang L L, Zhu H F, Wu P (2009). Reconstructing mean maximum temperature of growing season from the maximum density of the Schrenk Spruce in Yili, Xinjiang, China. Chin Sci Bull, 54(13): 2300–2308

Cinnirella S, Magnani F, Saracino A, Borghetti M (2002). Response of a mature *Pinus laricio* plantation to a three-year restriction of water supply: structural and functional acclimation to drought. Tree Physiol, 22(1): 21–30

Comprehensive Expedition of Chinese Academy of Sciences in Xinjiang (1958). Comprehensive Investigation Report in Xinjiang. Beijing: Science Press, 1–24 (in Chinese)

Cook E R (1985). A time series analysis approach to tree-ring standardization. Dissertation for the Doctoral Degree. Tucson: University of Arizona, 1–171

Cook E R, Buckley B M, D'Arrigo R D, Peterson M J (2000). Warm-season temperatures since 1600 BC reconstructed from Tasmanian tree rings and their relationship to large-scale sea surface temperature anomalies. Clim Dyn, 16(2–3): 79–91

Cook E R, Kairiukstis L A (1990). Methods of Dendrochronology: Applications in the Environmental Sciences. Dordrecht: Kluwer Academic Publishers, 1–13

Dewar R C, Ludlow A R, Dougherty P M (1994). Environmental influences on carbon allocation in pines. Ecol Bull, 43: 92–101

Duan J P, Wang L L, Li L, Chen K L (2010). Temperature variability since A.D. 1837 inferred from tree-ring maximum density of *Abies fabric* in Gongga Mountains, China. Chin Sci Bull, 55(26): 3015–3022

Fan Z X, Bräuning A, Yang B, Cao K F (2009). Tree ring density-based summer temperature reconstruction for the central Hengduan Mountains in southern China. Global Planet Change, 65(1–2): 1–11

Greber G T, Chaloner W G (1984). Influence of environmental factors on the wood structure of living and fossil trees. Bot Rev, 50(4): 361–370

Gruber A, Strobl S, Veit B, Oberhuber W (2010). Impact of drought on the temporal dynamics of wood formation in *Pinus sylvestris*. Tree Physiol, 30(4): 490–501

He M H, Yang B, Datsenko N M (2014). A six hundred-year annual minimum temperature history for the central Tibetan Plateau derived from tree-ring width series. Clim Dyn, 43(3–4): 641–655

Irvine J, Perks M P, Magnani F, Grace J (1998). The response of *Pinus sylvestris* to drought: stomatal control of transpiration and hydraulic conductance. Tree Physiol, 18(6): 393–402

Jones H G (1998). Stomatal control of photosynthesis and transpiration. J Exp Bot, 49(Special S1): 387–398

Kite G W (1977). Frequency and Risk Analysis in Hydrology. Fort Collins: Water Resources Publication, 19–38

Lambers H, Chapin F S, Pons T L (2008). Plant Physiological Ecology (2nd ed). New York: Springer, 29–240

Lenz O, Schär E, Schweingruber F H (1976). Methodische probleme bei der radiographisch-densitometrischen Bestimmung der Dichte und der Jahrringbreiten von Holz. Holzforschung, 30(4): 114–123

Lu P, Yan G X (1990). Xinjiang Forest. Beijing: China Forestry Publishing House, 94–235 (in Chinese)

Luckman B H, Briffa K R, Jones P D, Schweingruber F H (1997). Tree-ring based reconstruction of summer temperatures at the Columbia Icefield, Alberta, Canada, AD 1073−1983. Holocene, 7(4): 375–389

Miedes E, Zarra I, Hoson T, Herbers K, Sonnewald U, Lorences E P (2011). Xyloglucan endotransglucosylase and cell wall extensibility. Journal of plant physiology, 168(3): 196–203

Nemhauser J L, Hong F X, Chory J (2006). Different plant hormones regulate similar processes through largely nonoverlapping transcriptional responses. Cell, 126(3): 467–475

Pant G B, Kumar K R, Borgaonkar H P, Okada N, Fujiwara T, Yamashita K (2000). Climatic response of *Cedrus deodara* tree-ring parameters from two sites in the western Himalaya. Can J Res, 30(7): 1127–1135

Pichler P, Oberhuber W (2007). Radial growth response of coniferous forest trees in an inner Alpine environment to heat-wave in 2003. For Ecol Manage, 242(2–3): 688–699

Piovesan G, Biondi F, Di Filippo A, Alessandrini A, Maugeri M (2008). Drought-driven growth reduction in old beech (*Fagus sylvatica*) forests of the central Apennines, Italy. Glob Change Biol, 14(6): 1265–1281

Schweingruber F H, Bartholin T, Schaur E, Briffa K R (1988). Radiodensitometric-dendroclimatological conifer chronologies from Lapland (Scandinavie) and the Alps (Switzerland). Boreas, 17(4): 559–566

Schweingruber F H, Briffa K R, Jones P D (1991). Yearly maps of summer temperatures in western Europe from A.D. 1750 to 1975 and western North America from 1600 to 1982: results of a radio-densitometrical study on tree rings. Vegetatio, 92(1): 5–71

Shao X M, Xu Y, Yin Z Y, Liang E Y, Zhu H F, Wang S (2010). Climatic implications of a 3585-year tree-ring width chronology from the northeastern Qinghai-Tibetan Plateau. Quat Sci Rev, 29(17–18): 2111–2122

Shi Y G (2006). China's Meteorological Disaster Records: Xinjiang Volume. Beijing: China Meteorological Press, 11–196 (in Chinese)

Swarup K, Benkova E, Swarup R, Casimiro I, Péret B, Yang Y, Parry G, Nielsen E, De Smet I, Vanneste S, Levesque M P, Carrier D, James N, Calvo V, Ljung K, Kramer E, Roberts R, Graham N, Marillonnet S, Patel K, Jones J D G, Taylor C G, Schachtman D P, May S, Sandberg G, Benfey P, Friml J, Kerr I, Beeckman T, Laplaze L, Bennett M J (2008). The auxin influx carrier LAX3 promotes lateral root emergence. Nat Cell Biol, 10(8): 946–954

Uggla C, Magel E, Moritz T, Sundberg B (2001). Function and dynamics of auxin and carbohydrates during earlywood/latewood transition in scots pine. Plant Physiol, 125(4): 2029–2039

Wang X C, Li Z S, Ma K P (2014). Decreased sensitivity of tree growth to temperature in Southeast China after the 1976/'77 regime shift in Pacific climate. Sains Malaysiana, 43(1): 9–19

Wiley E, Helliker B (2012). A re-evaluation of carbon storage in trees lends greater support for carbon limitation to growth. New Phytol, 195(2): 285–289

Wimmer R, Grabner M (2000). A comparison of tree-ring features in *Picea abies* as correlated with climate. International Association of Wood Anatomists Journal, 21(4): 403–416

Yang B, Qin C, Wang J L, He M H, Melvin T M, Osborn T J, Briffa K R (2014). A 3,500-year tree-ring record of annual precipitation on the northeastern Tibetan Plateau. Proc Natl Acad Sci USA, 111(8): 2903–2908

Yasue K, Funada R, Kobayashi O, Ohtani J (2000). The effects of tracheid dimensions on variations in maximum density of *Picea glehnii* and relationships to climatic factors. Trees (Berl), 14(4): 223–229

Yuan M, Shaw P J, Warn R M, Lloyd C W (1994). Dynamic reorientation of cortical microtubules, from transverse to longitudinal, in living plant-cells. Proc Natl Acad Sci USA, 91(13): 6050–6053

Yuan Y J, Shao X M, Wei W S, Yu S L, Gong Y, Trouet V (2007). The potential to reconstruct Manasi River streamflow in the northern Tien Shan mountains (NW China). Tree-Ring Research, 63(2): 81–93

Zhang T W, Zhang R B, Yuan Y J, Gao Y Q, Wei W S, Diushen M, He Q, Shang H M, Wang J (2015). Reconstructed precipitation on a centennial timescale from tree rings in the western Tien Shan Mountains, Central Asia. Quaternary International, 358: 58–67

Zhang X W (2006). Xinjiang Meteorological Manual. Beijing: China Meteorological Press, 1–506 (in Chinese)

Zhu H F, Fang X Q, Shao X M, Yin Z Y (2009). Tree ring-based February-April temperature reconstruction for Changbai Mountain in Northeast China and its implication for East Asian winter monsoon. Clim Past, 5(4): 661–666